

INTERNATIONAL SOCIETY FOR SOIL MECHANICS AND GEOTECHNICAL ENGINEERING



This paper was downloaded from the Online Library of the International Society for Soil Mechanics and Geotechnical Engineering (ISSMGE). The library is available here:

<https://www.issmge.org/publications/online-library>

This is an open-access database that archives thousands of papers published under the Auspices of the ISSMGE and maintained by the Innovation and Development Committee of ISSMGE.

The paper was published in the proceedings of the 12th Australia New Zealand Conference on Geomechanics and was edited by Graham Ramsey. The conference was held in Wellington, New Zealand, 22-25 February 2015.

Relationship between water retention, stiffness and damping ratio in soils

Z.Y. Cheng¹, and E. C. Leong².

¹School of Civil and Environmental Engineering, Nanyang Technological University, Block N1, 50 Nanyang Avenue, Singapore 639798; email: zcheng003@e.ntu.edu.sg

²School of Civil and Environmental Engineering, Nanyang Technological University, Block N1, 50 Nanyang Avenue, Singapore 639798; PH (+65) 6790-4774; email: cecileong@ntu.edu.sg

ABSTRACT

Today, geotechnical designs are facing more stringent and challenging criteria. Parameters like the small-strain stiffness and damping ratio of soil are now deemed necessary for design. While determination of small strain stiffness using wave propagation techniques are well established, determination of damping ratio remains largely elusive. This paper aims to investigate the effect of varying water content and stiffness on the wave velocities and damping ratio of soil. Experiments were conducted in a modified triaxial test setup. Variation in water content was achieved by using the axis-translation technique to apply matric suction on the soil specimen following the water retention curve of the soil. Upon equilibrium at the respective water contents, P and S waves were transmitted and received using the bender/extender elements located at both ends of the specimens. Wave velocities were calculated from the travel time while the damping ratios were derived using the Hilbert transform method. The experiment was repeated on similar soil specimens at different confining pressures. These experimental results were further verified with finite element modelling using the viscoelastic model in LS-DYNA. Successful implementation and verification of the technique using S waves not only allows more accurate determination of small-strain parameters on relatively undisturbed specimens, it also enables the determination of these parameters in-situ using seismic survey methods such as P-S logging.

Keywords: Damping ratio, P-wave, S-wave, Hilbert transform, Bender element

1 INTRODUCTION

Today, the prevalence of challenging construction coupled with more stringent design criteria meant that conventional parameters like the friction angle and cohesion intercept are no longer sufficient for geotechnical design. Engineers now need to account for transient and seismic loadings thereby requiring design parameters like small-strain soil stiffness and damping ratio. This explains the prevalence of advanced geotechnical testing using the resonant column test, cyclic triaxial, dynamic simple shear and the bender element tests. Except for the bender element tests, most of the mentioned advanced geotechnical tests are able to obtain both small-strain soil stiffness and damping ratio although at different range of small strains.

The bender element test has gained popularity rapidly in recent years due to its versatility and compact size. By incorporating bender elements into commonly available geotechnical testing equipment like the triaxial apparatus, small-strain soil stiffness can be obtained through the wave travel-time method. Meanwhile, conventional testing can still be conducted in the process thereby more information can be obtained from a single soil specimen. By altering the wiring configuration, both P and S-wave signals can be obtained from the bender elements (Lings and Greenings 2001, Leong et al. 2009) to give the small-strain bulk and shear moduli. Despite the above-mentioned advantages, one major short-coming of the bender element test is its inability to provide the material damping ratio.

Cheng and Leong (2014) attempted to use the Logarithmic Decrement method (ASTM D4015-07 2007) and the Spectral Ratio Method (Toksöz et al., 1979) in the bender element tests to obtain the material damping ratio. The Logarithmic Decrement Method (LDM) requires high quality signals unaffected by interference from reflected waves. However, the interference from reflected waves is dependent on the excitation frequency and high quality signals are difficult to obtain. The Spectral Ratio Method (SRM) compares the amplitudes of the signals from identical specimens of different

lengths i.e. different distance of wave propagation. However it is difficult to obtain two identical specimens in practice. Furthermore, SRM assumes that the contact conditions in the two tests are identical which are most often not the case. As such, values of damping ratio obtained were inconsistent and showed great amount of scatter.

The objective of this paper is study the relationship of water retention, stiffness and damping ratio of soils through bender element tests. The Hilbert transform method is introduced as a better alternative to LDM and SRM to obtain the material damping ratio from the bender element tests. Primary (P) and shear (S) waves are studied. Variation of the damping ratio and wave velocities with varying water content and soil stiffness are studied. The finite-element program LS-DYNA was used to verify the Hilbert Transform method to obtain the material damping ratio.

2 THE HILBERT TRANSFORM METHOD

The Hilbert transform is an operator which convolutes a signal by $1/\pi x$. In other words, it is a filter which transforms the signal by shifting their phases by $\pm\pi/2$ while maintaining the magnitudes of their respective spectral components. It was first used by Agneni and Balis-Crema (1986) to derive damping ratio in composite materials. However, most signals by nature consist of numerous frequency components which can affect the Hilbert transform of the time signal. Huang et al. (1998) later incorporated the 'empirical mode decomposition' method which helps to decompose complicated signals into their respective modal component to yield well-behaved Hilbert transforms. This method was later employed by Salvino (2000), Zhang and Tamura (2003), Yang et al. (2004) to investigate damping in structures like tall building from forced vibration responses like wind loading. This method is suitable for bender element tests as the signals generated by the bender elements are transient in nature and therefore are expected to decay in a free-vibration manner. For completeness, the derivation of material damping using the Hilbert transform (Salvino 2000, Iglesias 2000) is reproduced below.

If $x(t)$ is the signal in the time domain (Equation 1a) and $x^H(t)$ is the Hilbert transform of the time domain signal (Equation 1b), the combination will give the analytic signal $x_a(t)$ as shown below

$$x(t) = Ae^{-\xi\omega_n t} \sin(\omega_n t \sqrt{1-\xi^2}) \quad (1a)$$

$$x^H(t) = Ae^{-\xi\omega_n t} \cos(\omega_n t \sqrt{1-\xi^2}) \quad (1b)$$

$$x_a(t) = x(t) - ix^H(t) \quad (1c)$$

where A is the amplitude of the signal, ξ is the damping ratio, ω_n is the natural radian frequency, t is the time in seconds and i is the imaginary number

The magnitude of the analytic signal gives the envelope of the time signal $x_a(t)$ (Equation 2) i.e., eliminating the oscillatory components. By taking natural logarithm on both sides of Equation (2), the damping ratio ξ can be separated as shown in Equation (3)

$$|x_a(t)| = Ae^{-\xi\omega_n t} \quad (2)$$

$$\ln(|x_a(t)|) = \ln(A) - (\xi\omega_n)t \quad (3)$$

Equation (3) shows that the gradient used to derive the damping ratio from the plot of $\ln(|x_a t|)$ with time has to be downwards sloping. The damping ratio can be derived from the gradient as shown in Equation (4). Further information on the procedures to process the received signal is elaborated later.

$$\xi = \frac{m}{\omega_n} = \frac{m}{2\pi f_n} \quad (4)$$

where m is the gradient and f_n is the natural frequency of the signal.

3 EXPERIMENT SETUP AND PROCEDURES

River sand was used in this study. The sand has a specific gravity of 2.65, maximum void ratio of 0.89 and minimum void ratio of 0.5. Relative density of the sand specimens was around 80%. The grain size distribution curve is shown in Figure 1.

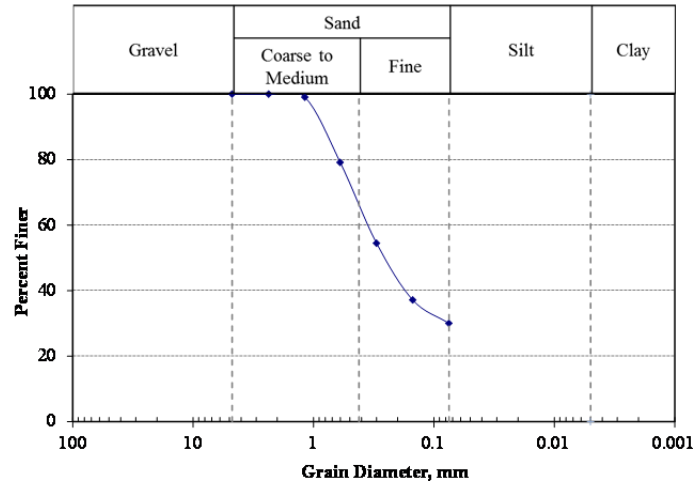


Figure 1. Grain size distribution curve of river sand

Sand specimens with height and diameter of 50 mm were reconstituted using the moist tamping method. Moist sand at 15% water content was prepared and then placed in lifts of 10 mm into a brass split mould with an internal diameter of 50 mm. Each lift was tamped 50 times using a 25 mm diameter metal rod. The top surface of each lift was lightly scarified to ensure good bonding between lifts. The specimens prepared have a void ratio ranging from 0.51 to 0.55.

The sand specimens were tested at net normal stresses ($\sigma_3 - u_a$) of 200 and 400 kPa where σ_3 is confining pressure and u_a is pore-air pressure. Specimen tags for the respective specimens are RS-US_200 and RS-US_400. The experiment set-up is similar to that illustrated in Cheng & Leong (2013) except that the ultrasonic platens were replaced with bender elements. The sand specimens were initially saturated with application of a back pressure. Saturation was deemed completed when the B-value was greater than 0.95 or when P wave velocity (V_p) was about 1500 m/s. Once the sand specimen was fully saturated, matric suction was applied. Different matric suction ($u_a - u_w$) conditions were achieved by maintaining the pore-air pressure (u_a) constant while reducing the pore-water pressure (u_w). The water retention curve was obtained by monitoring the water content of the soil specimen during the test.

At each matric suction, the bender element was excited with a single sinusoidal pulse of 3, 5, 10, 20 and 50 kHz in both flexure and extender modes. Signals were recorded at a sampling frequency of 2 MHz and for a duration of 5 ms. The wave velocity was computed by dividing the tip-to-tip distance of the bender elements by the travel time. Generally the S-wave signals were stronger when excited at lower frequencies of 3, 5, 10, 20 kHz while P-wave signals were stronger when excited at higher frequencies of 10, 20 and 50 kHz. Signal strength of the bender elements was also affected by excitation voltage, contact condition and net confining stress (e.g. Leong et al. 2009). Only S-wave signals were analysed for material damping.

A MATLAB script was written to process the signals for different excitation frequencies. Signals were first passed through a fourth order Butterworth band-pass with lower and upper frequencies of 0.5 and 100 kHz, respectively. This is to remove any low frequency electrical drift which will affect the derivation of the damping ratio. The signals at various frequencies and matric suctions were studied to determine the natural frequency of the S wave. It was found that regardless of the net normal stress, matric suction and excitation frequency, the S-wave signal shows a peak at 2 kHz (Figure 2). This peak was the strongest when the specimen was excited at 3 kHz and its intensity reduced when excitation frequency increases beyond 3 kHz. The higher frequencies present in the signals were a result of the excitation pulse and the reflected waves.

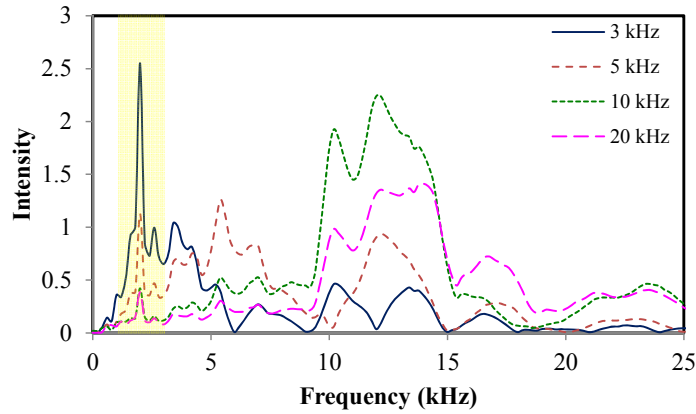


Figure 2. Typical frequency domain of S wave signals at different excitation frequencies ($u_a-u_w=10kPa$)

The natural frequency of the bender element system at 2 kHz was confirmed with the help of the finite element program, LS-DYNA. A specimen of identical dimensions was simulated using implicit eigenvalue analysis to derive the natural frequency at the various modes of vibration. Bulk and shear stiffnesses derived from the P- and S-wave velocities (V_p and V_s) together with the bulk density were input into the elastic material model. The natural frequencies in the bending mode for the fixed-free and fixed-fixed mode of a cylindrical soil specimen were found to be 1 and 2.6 kHz, respectively. Since the boundary condition of the specimen lies between those of fixed-free and fixed-fixed condition, it was expected to fall between 1 and 2.6 kHz and thus, the experimental results gave good agreement.

With the natural frequency of the bender element system determined, a time window was applied to the filtered signal to retain only values from 2 to 5 ms so as to eliminate the effect of the excitation pulse and the reflected waves. The windowed signal was then passed through another fourth order Butterworth low-pass filter with an upper frequency of 3.5 kHz. Hilbert transform was then applied to obtain the plot described in Equation (3). A best-fit line was then constructed through a smaller time window (2.5 – 4.5 ms) in order to obtain the gradient used for calculating the damping ratio.

4 DISCUSSIONS AND RESULTS

4.1 Water retention curves

The water retention curves for the soil at net normal stresses of 200 and 400 kPa are shown in Figure 3. Air-entry value for RS-US_200 and RS-US_400 are at 6.7 kPa and 9.6 kPa, respectively.

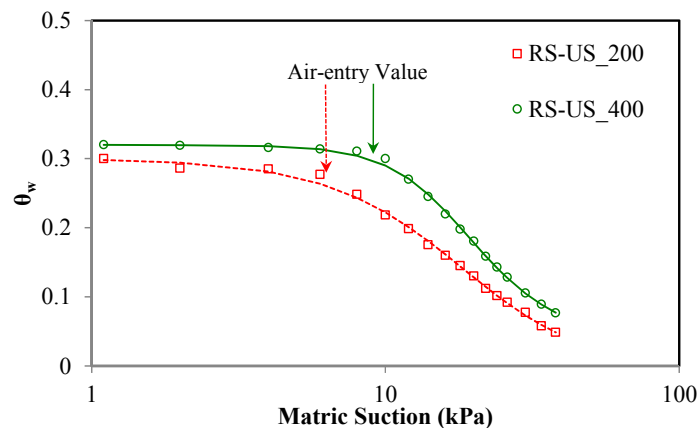


Figure 3. Water retention curve of soil specimens

4.2 V_p and V_s

P-wave velocity (V_p) was obtained as the specimen desaturates from full saturation as shown in Figure 4. At full saturation, V_p of the soil specimens was about 1600 m/s ($\approx V_p$ of water) and remained

constant up to the air-entry value. It started to decrease sharply after the air-entry value, demarcated by the dotted lines in Figure 4. After which, changes in V_p were minimal, varying within 2% of the mean (463 m/s). The degree of saturation corresponding to the drop in V_p values were at approximately 90%. This suggests that while V_p is sensitive to the degree of saturation, the effect is only observed around the air-entry value.

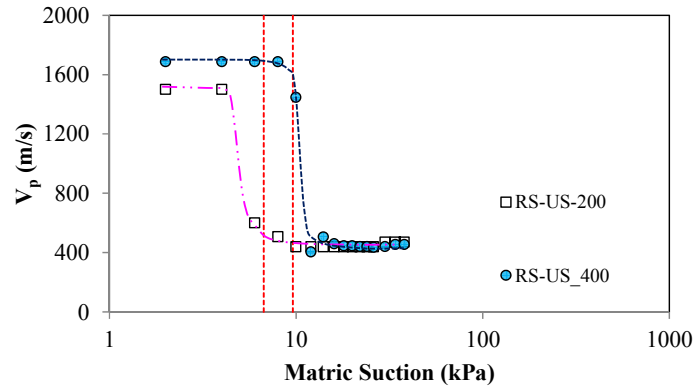


Figure 4. Variation of V_p with matric suction

On the other hand, S-wave velocity (V_s) was shown to increase as the soil specimens stiffened with increasing matric suction upon drying. The extent of increase was smaller for RS-US_400 due to the higher net normal stress.

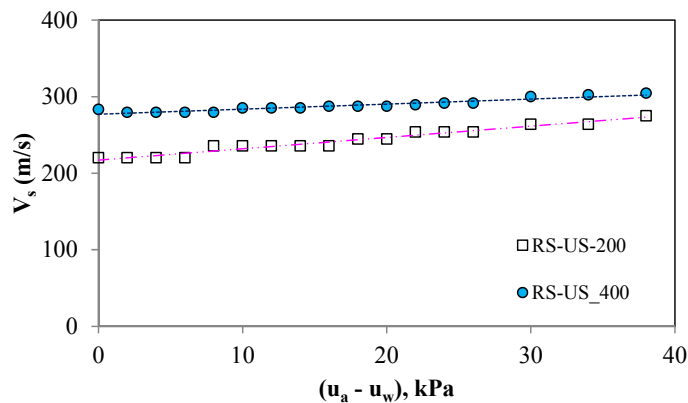


Figure 5. Variation of V_s with matric suction

4.3 Damping ratio

4.3.1 Simulation

Finite-element program, LS-DYNA, was used to model the bender element tests. LS-DYNA was used due to its ability to simulate both explicit and implicit analysis of transient dynamic problems. The soil specimen was modeled as a 3D cylinder with 35000 elements (Figure 6). An explicit time integration mode was used. A row of five nodes, corresponding to 5.3 mm, situated in the middle of the cross-section and at the top surface of the numerical model were chosen to excite in the transverse mode. The response was picked up at a node lying in the middle of the cross-section, 4 mm from the bottom end. The bottom end of the model was fixed from translational and rotational movement.

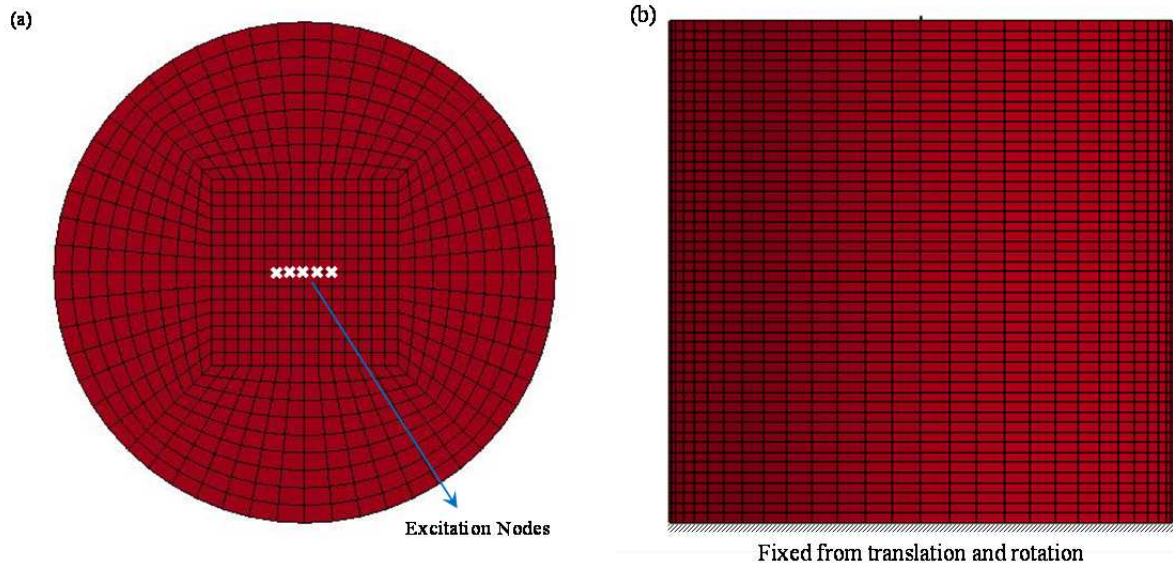


Figure 6.(a) Top and (b) front view of finite element model

Excitation frequencies of 5 and 10 kHz were used. Using the viscoelastic model, damping ratios of 0.03 and 0.07 were assigned to the model for each of the excitation frequency. Figure 7a shows the raw and processed S-wave signals in the time domain for the simulation excited at 5 kHz with a material damping of 0.03. They are then plotted in the frequency domain to ascertain that the signal processing did not filter out the natural frequency (Figure 7b). The magnitude of the simulated S-wave signal with time together with the best-fit line was shown in Figure 7c. The input damping ratios are compared with those derived from the Hilbert transform method in Table 1.

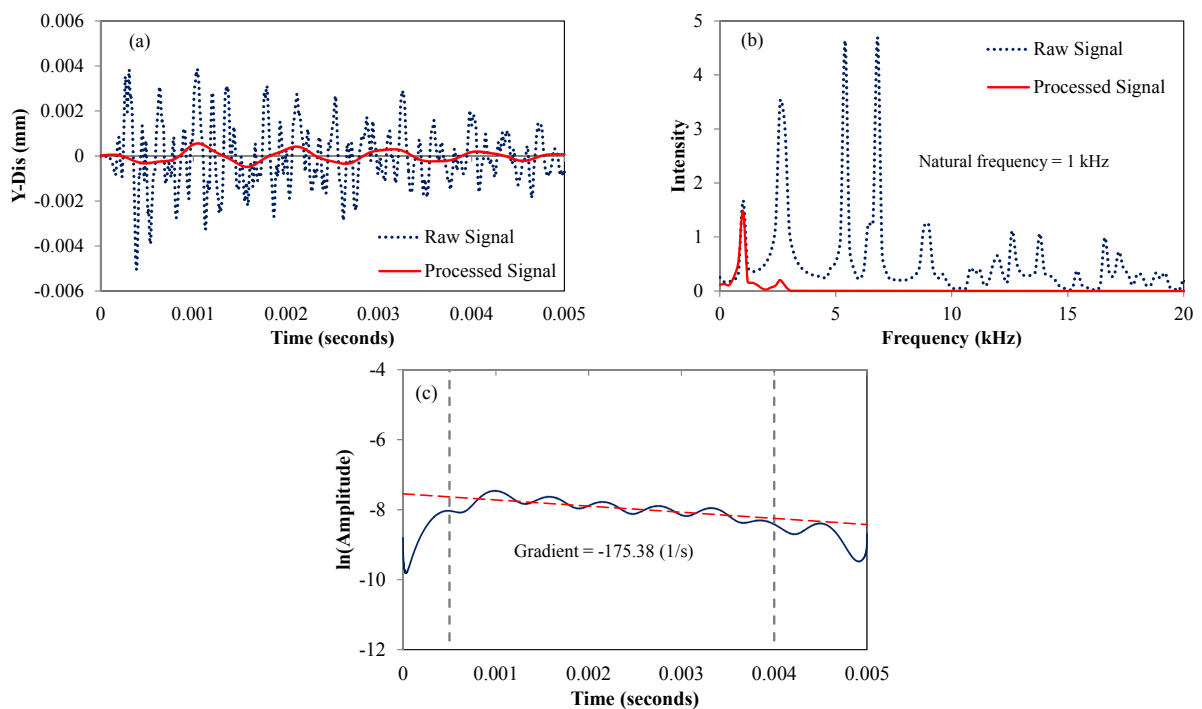


Figure 7. (a) Time domain, (b) frequency domain and (c) Hilbert transform of the simulated signal

Differences between the input damping ratio and those derived from Hilbert transform method are within $\pm 10\%$. The procedures described have proven to be feasible in deriving the damping ratio from a pulse excitation.

Table 1: Comparison between input damping ratio and those derived from HTM

Excitation Frequency (kHz)	Input ξ	ξ from HTM	Difference (%)
3	0.03	0.0279	6.96
	0.07	0.0760	-8.51
10	0.03	0.0312	-4.15
	0.07	0.0735	-5.03

4.3.2 Experiment results

The Hilbert transform method was applied on S-wave signals obtained for different excitation frequencies (3, 5, 10 and 20 kHz) and the damping ratios are shown in Figures 8 and 9 for specimens RS_US_200 and RS_US_400, respectively. Range of the damping ratio is approximately similar for both specimens. As the specimens stiffen during desaturation, the damping ratio is seen to decrease as the stiffer specimen is a better medium for wave propagation. The trend was especially evident in Figures 8. Figure 9 shows that the damping ratio increases slightly back up after the initial drop before plateauing.

Although it seems that the excitation frequency does not affect the damping ratios in Figures 8 and 9, it does to a great extent affect the quality of signal. It can be observed, upon close scrutiny, that the scatter of the damping ratio is larger when excitation frequency deviates from the natural frequency of the system. In Figure 8, damping ratios from excitation frequency of 10 kHz were seen to scatter around the trend line drawn. The damping ratios at excitation frequency of 20 kHz showed some negative values and hence were not plotted in Figure 8. The scatter in damping ratios is due to the decrease in intensity of the vibration at 2 kHz as excitation frequency increases (see Figure 2). The extent of scattering at higher excitation frequencies was much lesser in Figure 9 since the stiffer specimen allows for better transmission of wave signals.

The above observations suggest that while damping ratios can be obtained from bender element tests using the Hilbert transform method, a range of excitation frequency should be used to determine the optimal frequency for high quality signals. A rough estimate of the optimal frequency could be obtained by determining the flexure mode natural frequency for the specimen.

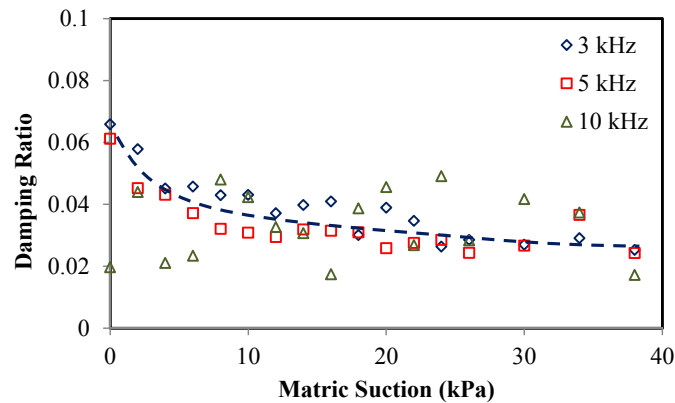


Figure 8. Variation of S-wave damping ratio with matric suction for RS-US_200

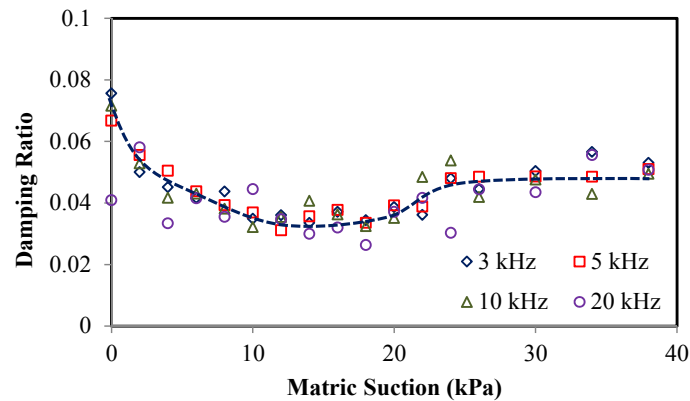


Figure 9. Variation of S-wave damping ratio with matric suction for RS-US_400

5 CONCLUSION

In this paper, variation of P and S-wave velocities and damping ratios with water content for a reconstituted sand were investigated. The P-wave velocity was shown to decrease abruptly after the air-entry value ($S_r \approx 90\%$). The S-wave velocity was shown to increase linearly as matric suction increases i.e., as degree of saturation decreases. The Hilbert transform method was introduced as an alternative means to obtain damping ratio from S-wave signals. The Hilbert transform method was shown to provide reliable estimates of the damping ratio.

6 ACKNOWLEDGEMENTS

The first author is a recipient of the Nanyang President Graduate Scholarship. The financial support from grant MINDEF-NTU-JPP/13/01/02 administered by the Protective Technology Research Center, Nanyang Technological University, is gratefully acknowledged.

REFERENCES

- Agneni, A. and Balis-Crema, L. (1986). "Damping measurements by Hilbert transform on composite materials." Damping Proceedings Volume 2, Las Vegas, Nevada, United States, F11-F113
- ASTM (2007). "D4015-07: Standard test methods for modulus and damping of soils by resonant-column method." ASTM International, West Conshohocken, PA, USA.
- Cheng, Z.Y. and Leong, E.C. (2013). "Ultrasonic testing of un-saturated soil." Springer Series in Geomechanics and Geo-engineering 2013: Multiphysical Testing of Soils and Shales, 105-110.
- Cheng, Z.Y. and Leong, E.C. (2014). "Effect of confining pressure and degree of saturation on damping ratios of sand." Proceedings of the 6th International Conference on Unsaturated Soils UNSAT2014, Sydney, Australia, 277-282
- Huang, N.E., Shen, Z., Long, S.R., Wu, M.C., Shih, H.H., Zheng, Q., Yen, N.C., Tung C.C. and Liu, H.H. (1998). "The empirical mode decomposition and the Hilbert spectrum for nonlinear and non-stationary time series analysis." Proceedings of the Royal Society of London. Series A: Mathematical, Physical and Engineering Sciences, 454(1971), 903-995.
- Iglesias, A.M. (2000). "Investigating various modal analysis extraction techniques to estimate damping ratio." MSc Dissertation, Virginia Polytechnic Institute and State University, United States
- Leong, E.C., Cahyadi, J. and Rahardjo, H. (2009). "Measuring shear and compression wave velocities of soil using bender-extender elements." Canadian Geotechnical Journal, 46(7), 792-812.
- Lings, M.L. and Greening, P.D. (2001). "A novel bender/extender element for soil testing." Geotechnique, 51(8), 713-717
- Salvino, L.W. (2000). "Empirical mode analysis of structural response and damping." Proceedings of the 18th International Modal Analysis Conference, San Antonio, Texas, United States, 503-509
- Toksöz, M.N., Johnston, D.H. and Timur, A. (1979). "Attenuation of seismic waves in dry and saturated rocks: I. Laboratory measurements." Geophysics, 44(4), 681-690.
- Yang, J.N., Lei, Y., Lin, S. and Huang, N. (2004). "Identification of natural frequencies and dampings of in situ tall buildings using ambient wind vibration data." Journal of engineering mechanics, 130(5), 570-577.
- Zhang, L., and Tamura, Y. (2003). "Damping estimation of engineering structures with ambient response measurements." Proceeding of the 21st International Modal Analysis Conference, Kissimmee, Florida, United States